Diffraction separation using the CRS technique: A field data application

Endrias G. Asgedom, and Leiv -J. Gelius (University of Oslo, Center for Imaging and Department of Geosciences, Norway)
Martin Tygel (State University of Campinas, Department of Applied Mathematics, Brazil)

Abstract

Diffracted waves are often associated with geological structures like faults, pinchouts, wedgeouts or a sudden change in facies (Kanasewich and Phadke, 1988). Identification of such structures in a seismic or ground penetrating radar (GPR) image is highly dependent on our ability to utilize the diffracted energy. Unfortunately, diffractions often manifest themselves on seismic (or GPR) data with a much weaker signal strength compared to reflections and they often fall within the noise level. As a consequence, classical signal processing methods treat diffractions as noise and imaging is carried out in favor of reflections. Recently, however, different approaches have been proposed to separate diffractions from reflections so that additional high-resolution information can be obtained from direct imaging of the diffracted energy.

In this paper, we propose to perform diffraction and reflection separation based on the Common Reflection Surface (CRS) concept. Within this formulation, suppression (or attenuation) of reflections is carried out by selecting the appropriate stacking surface for diffractions based on a coherency measure. Here we tested both Semblance and MUltiple SIgnal Classification (MUSIC) as a coherency measure for the CRS parameter estimation. The potential application of the technique has been demonstrated employing a multi-offset GPR dataset.

Introduction

Imaging of possible hydrocarbon traps like faults and unconformities (especially their accurate locations) is a very important task in exploration (Kanasewich and Phadke, 1988; Zhang, 2004). Most of the location information of such structural hydrocarbon traps is embedded in the diffracted wave energy (Taner et al., 2006; Fomel et al., 2007; Moser and Howard, 2008). As a consequence, traditional seismic or GPR imaging schemes, tailored for reflections, generally suffer in quality and resolution (Neidell, 1997). To overcome this problem many recent attempts have been made to separate diffractions from reflections and accordingly use them to obtain a higher resolved image of discontinuities.

Landa et al. (1987) proposed the use of a specialized double-square-root traveltime moveout, so as to enhance diffractions and attenuate reflections by stacking. Fomel and co-workers (2002, 2007) introduced plane-wave destruction filters to separate diffractions after stack and use them within migration velocity analysis. Moser and Howard (2008) used the concept of anti-stationary filtering to perform depth imaging of diffractions.

In this paper we follow the basic idea of Landa et al (1987) in the framework of the Common Reflection Surface (CRS) technique. Standard use of CRS enhances the image quality based on reflection data. However, within the same formulation a moveout equation can be constructed which will enhance diffractions instead of reflections. Hence, an optimal diffraction stack can potentially be obtained where all reflections have been efficiently suppressed.

CRS diffraction stack surface

CRS stacking is a method that utilizes multi-coverage data to simulate Zero Offset (ZO) seismic or GPR sections. In case of reflections the inherent stacking operator (or traveltime moveout) depends on two wavefield concepts: (i) the wavefront associated with the Normal Incidence Point (NIP) generated by a point source in depth and (ii) the Normal (N) wavefront corresponding to an exploding reflector type of source. According to this formulation, seismic or GPR events are assumed to be well approximated by the generalized hyperbolic equation. More specifically, the CRS moveout of the reflection event, w, is specified by the zero-offset (ZO) traveltime, τ_{0_w}, and (reference) trace location, x_{0_w}. In the 2D situation, it is given by

$$[\tau_w^\theta(x_m,h)]^2 = [\tau_{0_w} + A_w(x_m - x_{0_w})]^2 + B_w(x_m - x_{0_w})^2 + C_w h^2 \ , \quad (1)$$

where (x_m, h) are the midpoint and half-offset coordinate of a source-receiver pair in the vicinity of the reference location. Moreover,

$$\theta = \{A_w, B_w, C_w\} \ , \quad (2)$$

is the CRS parameter vector, with three parameters, A_w, B_w and C_w, to be estimated from the data.

In case the recorded data stems from a diffraction, the condition $B_w = C_w$ holds. This is because, as the reflector shrinks to a point, the N-wave turns out to be identical to the NIP-wave (Zhang et. al., 2001). As a consequence, the hyperbolic moveout of diffractions (or *diffraction traveltime*), reduces to,

$$[\tau_w^\theta(x_m,h)]^2 = [\tau_{0_w} + A_w(x_m - x_{0_w})]^2 + B_w[(x_m - x_{0_w})^2 + h^2] \ . \quad (3)$$

Direct comparison between Eqs. (1) and (3) demonstrate that the reflections and diffractions follow different traveltime curves. Hence, in order to enhance the diffracted contributions relative to those being reflected, the CRS stacking should be carried out based on Eq. (3). However, to ensure that optimal CRS parameters are determined corresponding to the best fitting between the CRS traveltime moveout and the actual diffraction event(s) present in the measurements, a coherency measure has to be employed.

Coherency measures for CRS stacking

Classically, coherency measures in seismic or GPR is performed based on Semblance. Even though, Semblance is the most robust algorithm, it has resolution problems when it comes to closely interfering events (Biondi and Kostov, 1989). In order to overcome this problem, higher resolution methods like MUSIC have been proposed (Biondi and Kostov, 1989; Kirlin, 1992). Here we briefly review both Semblance and MUSIC and perform coherency measures for selecting the optimum diffraction stacking surface.

Semblance

Following Du and Kirlin (1993), Semblance can be formulated in terms of the covariance matrix of the data. Within a selected time window along the chosen trial moveout, Semblance has the mathematical expression

$$S_c = \frac{\mathbf{u}^T \mathbf{R}(\theta)\mathbf{u}}{Mtr(\mathbf{R}(\theta))} \ , \tag{4}$$

where $\mathbf{u}$ is a column vector of ones, which can be referred to as the *unitary steering* vector, and $\mathbf{R}(\theta)$ is the *steered* covariance matrix (or the covariance computed witin a window following the defined traveltime trajectory). Here θ is the vector containing all the parameters of the traveltime (compare with equation 2). As in usual notation, $E\{\}$ and $tr()$ represent the expected value and matrix trace, respectively. Moreover, superscript T represents transpose. Equation (4) provides the interpretation that Semblance can be regarded as a normalized output/input energy ratio within the selected time window.

MUSIC

The basic idea behind subspace methods like MUSIC is to decompose the data covariance matrix into two orthogonal subspaces: (i) the signal subspace spanned by the eigenvectors associated with large eigenvalues and (ii) the noise subspace spanned by the eigenvectors corresponding to small or zero eigenvalues. Mathematically, this eigendecomposition of the covariance matrix can be written as

$$\mathbf{R}(\theta) = \mathbf{V}_s(\theta)\Sigma_s(\theta)\mathbf{V}_s^H(\theta) + \mathbf{V}_n(\theta)\Sigma_n(\theta)\mathbf{V}_n^H(\theta) \ , \tag{5}$$

where $\mathbf{V}_s(\theta)$ and $\mathbf{V}_n(\theta)$ are the signal and noise subspace eigenvector matrices while $\Sigma_s(\theta)$ and $\Sigma_n(\theta)$ are the corresponding eigenvalue matrices, respectively. The mathematical decomposition of the covariance matrix in Eq. (5) has its physical decomposition counterpart. Assume that the different sources can be described by a zero-mean stochastic process and that the noise is white Gaussian with variance σ_n^2. The data covariance matrix is now given as

$$\begin{aligned} \mathbf{R}(\theta) &= E\{\mathbf{D}(\theta)\mathbf{D}(\theta)^H\} \\ &= \mathbf{U}\mathbf{R}_s(\theta)\mathbf{U}^H + \sigma_n^2\mathbf{I} \ , \end{aligned} \tag{6}$$

where $\mathbf{D}(\theta)$ is the data matrix containing all the data within a window, $\mathbf{R}_s(\theta)$ is the steered source covariance matrix, $\mathbf{U}$ and $\mathbf{I}$ are unitary and identity matrices, respectively. Finally, H denotes complex conjugate transpose. Note that in case of uncorrelated sources, the matrix $\mathbf{R}_s(\theta)$ will be diagonal.

In case of narrowband and uncorrelated signals, MUSIC exploits the fact that the "correct" moveout, represented as a steering vector, must lie in the signal subspace and therefore is orthogonal to the noise subspace eigenvectors. As a consequence, the projection of the steering vector onto the noise subspace provides a nearly vanishing value. The inverse of such a projection (namely the sum of the dot products of the steering vector with the noise eigenvectors) should peak when the steering vector represents a correct moveout. From this consideration the MUSIC measure of coherency (referred to as MUSIC pseudo-spectrum) is given by

$$\mathbf{P}_{MUSIC}(\theta) = \frac{\mathbf{u}\mathbf{u}^H}{\mathbf{u}\mathbf{P}_n(\theta)\mathbf{u}^H} \ , \tag{7}$$

where $\mathbf{P}_n(\theta) = \mathbf{V}_n(\theta)\mathbf{V}_n(\theta)^H$ is the steered noise subspace projection matrix.

Seismic or GPR signals are both wideband and highly correlated and therefore the original MUSIC algorithm needs to be modified accordingly before being applicable to such data. The consequence of having correlated sources is that there will be a rank deficiency in the source covariance matrix $\mathbf{R}_s(\theta)$ that will result in a mix of signal and noise subspaces. As a result, the algorithm will loose its power to peak at the appropriate set of estimated parameters. In order to handle correlated sources, spatial smoothing over the covariance matrix can be employed (Biondi and Kostov, 1989; Kirlin, 1992). The idea is to subdivide the array of N_r sensors into K identical overlapping subarrays of $N_r - K + 1$ receivers and then compute the covariance for all the subarrays and average the result. If the covariance matrix for subarray k is $\mathbf{R}_k$, the spatially smoothed covariance is given by

$$\mathbf{R}_K = \frac{1}{K}\sum_{k=1}^{K} \mathbf{R}_k \ . \tag{8}$$

To be able to implement spatial smoothing in seismic or GPR, one has to taper the data within a window following the event(s). The purpose of this tapering is to make the delay times of the event linear (which is the basic requirement behind spatial smoothing) (Biondi and Kostov, 1989). The other advantage of performing the analysis in a given window is to make the steering vectors, required for generating the MUSIC pseudo-spectrum, to be frequency independent. This allows us to handle wideband seismic or GPR data. Windowing the event can be interpreted as steering the covariance matrix before eigendecomposition and using unity steering vectors for generating the MUSIC pseudo-spectra (Kirlin, 1992).

GPR data analysis

The concept of diffraction separation based on CRS is tested using a near-surface multi-offset ground-penetrating

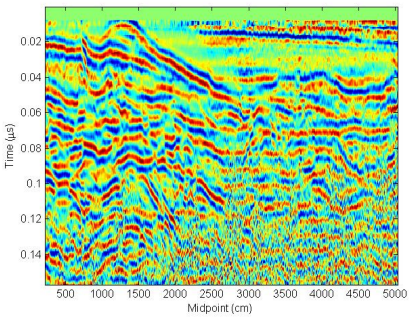

Figure 1: ZO section obtained from manually picked stacking velocities.

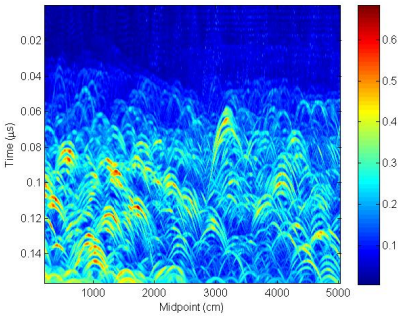

Figure 2: Coherency map of parameter A based on Semblance.

radar (GPR) dataset (Perroud and Tygel, 2005). The data is composed of 28 different offsets running every 0.2 m from 0.6 to 6 m. The CMP spacing is 0.1 m covering a 55-m-long profile.

The overall process is divided in to two steps: (i) perform velocity analysis for every CMP, where $x_m = x_{0_w}$, and determine parameter $C_w = 4/V_{rms}^2$, where V_{rms} is the root mean square velocity (in practice we assume that the stacking velocities resemble the rms-velocities well). Then, generate a ZO section using these velocities. (ii) setting $B_w = C_w$ and using a wide aperture search for parameter A_w in the ZO section, where $h = 0$. Both Semblance and MUSIC are used as coherency measures. Finally perform CRS stacking based on Eq. (3) and generate a diffraction-only ZO section.

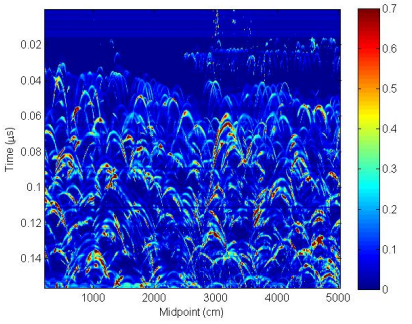

Figure 3: Coherency map of parameter A based on MUSIC.

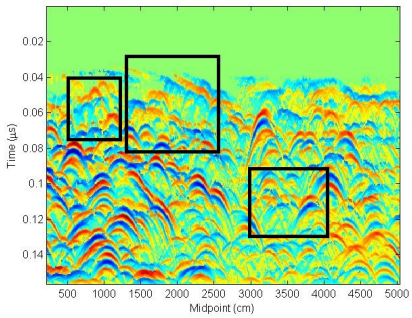

Figure 4: CRS diffraction stack based on Semblance.

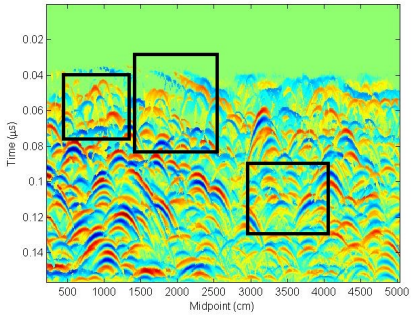

Figure 5: CRS diffraction stack based on MUSIC.

The stacking velocities required to generate the ZO section were obtained by means of Semblance computed within a window of 11 samples. Figure 1 shows the ZO section obtained where most of the diffractions are hidden behind the stronger reflection energy. Applying the CRS diffraction condition $B_w = C_w$ and using an aperture containing 40 traces, we then searched for parameter A_w. The coherency map corresponding to parameter A_w obtained from respectively Semblance and MUSIC are shown in Figures 2 and 3, respectively. The MUSIC coherency map represents the MUSIC pseudo-spectrum after being normalized by the energy of Semblance. The Semblance balancing is applied to condition the pseudo-spectrum since MUSIC gives unconstrained coherency values. Finally, we performed CRS stacking based on Eq. (3) using the parameters determined by Semblance (cf. Fig. 4) and MUSIC (cf. Fig. 5). In both cases diffractions are successfully separated from reflections and can then be used for further high-resolution imaging or velocity model building. In general, the result obtained using MUSIC is slightly better resolved and with less noise than that obtained by Semblance. This is especially noticeable within the three areas marked by black rectangles in Figs. 4 and 5.

Conclusions

A novel and highly robust approach to diffraction separation has been introduced and tested out. It is based on a generalized moveout equation valid for diffractions derived as a special case of the CRS moveout equation. The best possible separation between reflections and diffractions

requires the determination of the optimal CRS moveout parameters based on the use of a coherency measure. In this paper both Semblance and MUSIC were investigated. The proposed technique was applied to a multi-offset GPR dataset and demonstrated its potential to separate diffractions. Moreover, the use of MUSIC as a coherency measure gave an overall better resolved diffraction stack with less computational noise than in case of Semblance.

References

Kanasewich, E., and Phadke, S., 1988, Imaging discontinuities on seismic sections: Geophysics, vol. 53, No. 3, p334-345.

Zhang, R., 2004, Imaging the earth using seismic diffractions: CDSST annual report.

Fomel, S., 2002, Applications of plane-wave destruction filters: Geophysics, vol. 67, p1946-1960.

Fomel, S., Landa, E., and Taner, M.T., 2007, Poststack velocity analysis by separation and imaging of seismic diffractions: Geophysics, vol. 72, p89-94.

Landa, E., Shtivelman, V ., and Gelchinsky, B., 1987, A method for detection of diffracted waves on common-offset sections: Geophysical Prospecting, vol. 35, p359-373.

Taner, M.T., Fomel, S., and Landa, E., 2006. Separation and imaging of seismic diffractions using plane-wave decomposition: 76th SEG meeting, New Orleans, Louisiana, USA, Expanded Abstracts, 2401.

Moser ,T.J and Howard,C.B., 2008, Diffraction imaging in depth: Geophysical Prospecting, vol. 56, p627-641

Neidell, N. S., 1997, Perceptions in seismic imaging Part 2: Reflective and diffractive contributions to seismic imaging: The leading edge, p1121-1123

Zhang, Y., Bergler, S., and Hubral, P., 2001, Common-reflection-surface (CRS) stack for common offset: Geophysical Prospecting, vol. 49, p709-718.

Kirlin, R. L., 1992, The relationship between semblance and eigenstructure velocity estimators: Geophysics, vol. 57, p1027-1033.

Biondi, B., and Kostov, C., 1989, High-resolution velocity spectra using eigenstructure methods: Geophysics, vol. 54, p832-842.

Du, W. and Kirlin, R. L., 1993, Discrimination power enhancement via high resolution velocity estimators: IEEE Acoustics, Speech, and Signal Processing

Perroud, H., and Tygel, M., 2005, Velocity estimation by the common-reflection-surface (CRS) method: Using ground-penetrating radar data:Geophysics, vol. 70 No. 6, P. B43-B52.

Acknowledgments

The authors would like to thank Dr. Hevè Perroud for providing the GPR dataset.